Design and Implementation of a Small Scale Linear Switched Reluctance Motor

JY Lokamba, Nnamdi Nwulu and Kabeya Musasa
Dept. of Electrical and Electronic Engineering Science, University of Johannesburg, Auckland Park Kingsway Campus, Johannesburg, South Africa
nnwulu@uj.ac.za

Abstract

In this study, the working principles of a linear switched reluctance motor (LSRM) are demonstrated through the design and implementation of a linear switched reluctance motor with its appropriate control system. The paper focuses on merely demonstrating the working principles of the LSRM, and consequently does not focus on a specific application. A 6/4 poled, 3-phase LSRM is designed and implemented. The LSRM is controlled using a micro-controller and the accuracy of the control was improved by using linear incremental position sensors for feedback.

Keywords

Linear Switched Reluctance Motor, Speed control, linesar electric drives, electric drives control

1. INTRODUCTION

The LSRM finds itself applicable in many of the industrial applications, and it has started to gain popularity in recent years due to its reliability in harsh conditions and simplicity of construction. The LSRM can be used over a wide range of speeds, this flexibility allows the LSRM to be suitable in a number of application such as: Medical, elevators, locomotives and many more. However, the control of the LSRM is complex because of the nonlinear behaviour of the LSRM.

The LSRM is a suitable replacement of the linear induction or synchronous motors, because of the ease of manufacturing, reliability, good fault tolerance and lack of windings on the stator or the translator. The most commonly used motors in industrial applications are the induction and synchronous motor, the initial motion of these motors is rotational. Hence, in industrial applications where linear motion is needed, it is obtained by adding mechanical belts with pulleys and gearboxes. The addition of these components reduce the efficiency of the motor, as a result this supports the LSRM as a more attractive alternative in industrial applications that require linear motion.

In this paper, a detailed design of the LSRM is given. The design begins in the rotary domain and is then converted to the linear domain. The design is carried out in this manner because the rotational switched reluctance motor (RSRM) is the counterpart of the LSRM, thus the existing RSRM design methods can be extended to design the LSRM. Furthermore, the different control strategies are mentioned and a detailed explanation of the controller using the dsPIC33FJ16GS502 is given. The paper shall follow the following order: Section II presents the working principle of LSRM, section III the design equations of the LSRM, section IV the power electronic converter, and section V the control system and section VI is conclusions.

2. WORKING PRINCIPLE

The LSRM is obtained from its counterpart, the RSRM. For the RSRM, the number of stator poles is generally greater than that of the rotor poles, and the motors are characterized by the number of stator poles and rotor poles. For example, a RSRM of six stator poles and 4 rotor poles would be denoted as 6/4, other available combinations are 8/4, 8/6, 10/6 and so forth [1]. There are two types of configurations for the LSRM, namely the longitudinal flux and the transverse flux configurations. Both of the above mentioned configurations can be obtained from the RSRM by simply cutting it along its diagonal and unfolding the stator and rotor. The configurations of the LSRM are shown in Figure 1 and 2 below. The RSRM configuration is shown in Figure 3.

The windings of an LSRM can either be on the rotor or the stator, unlike the RSRM where the windings are only found on the stator [2]. Also, the LSRM can have an active stator and passive rotor or vice versa. The configuration with active stator has an advantage because the power converter and power supply are stationary, which results in less weight of the moving portion of the motor. The problem with this set up is that the number of required power converters increases, which increases the complexity and the cost [2].

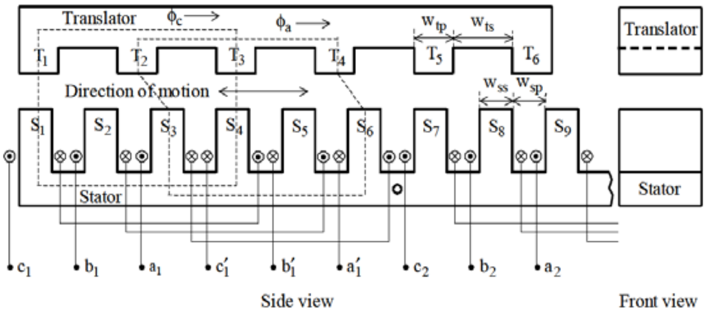

Figure 1: Longitudinal flux configuration

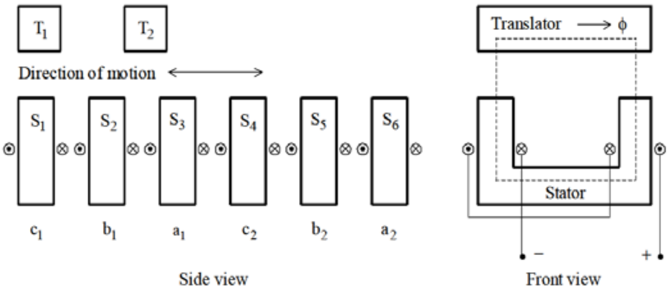

Figure 2: Transverse flux configuration

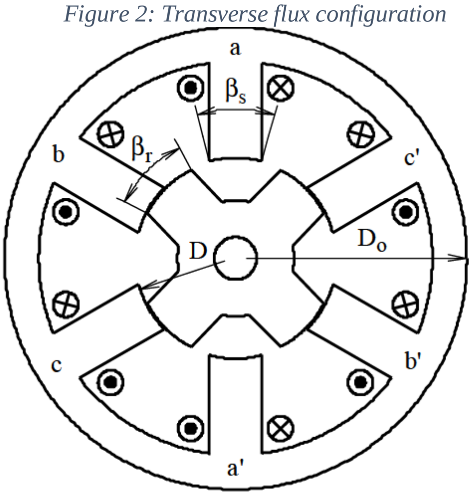

Figure 3: 6/4 three-phase RSRM

Linear motion is obtained from the LSRM by the tendency of the rotor to align itself with the excited stator. This is achieved by appropriately exciting the phases sequentially [3]. For instance, considere T_2, T_4, $S_3(a_1)$, and $S_4(a_2')$ from figure 1, where the T represents the translator poles and S the stator poles. When the phase winding a_1 is energized by passing a current through it, a flux will pass through the stator poles S_3 and S_4 as well as the translator poles T_2 and T_4. This generated flux causes the translator pole T_2 to move towards S_3 and T_4 to move towards S_4. Once they are aligned, the current through the phase is turned off. Hence, by knowing the position of the translator and exciting the phases accordingly, the desired motion is obtained. The reverse direction motion of the motor can be achieved by simply reversing the sequence of phase excitation. When the translator and stator pole are aligned, it is called the aligned position and this is the position of maximum phase inductance. The unaligned position is the position of minimum phase inductance, and it occurs when the translator pole is half a pitch away from the excited stator pole [2].

To understand the functionality of the LSRM i.e. how motion is achieved and how force is produced, one must understand the inductance profile of the motor. The inductance profile of a motor is dependent on motor parameters such as the stator and translator pole and slot widths, excitation currents and translator position [4]. The inductance profile is depicted in figure 4 below. Assuming that the inductance characteristics are independent of stator current excitation i.e. the magnetic circuit is linear, then a relationship between inductance and motor parameters can be derived [4]. The relationship is given by the following equations:

$$x_1 = \frac{w_{ts} - w_{sp}}{2} \tag{1}$$

$$x_2 = x_1 + w_{sp} = \frac{w_{ts} + w_{sp}}{2} \tag{2}$$

$$x_3 = x_2 + (w_{tp} - w_{sp}) = w_{tp} + \left(\frac{w_{ts} - w_{sp}}{2}\right) \tag{3}$$

$$x_4 = x_3 + w_{sp} = w_{tp} + \left(\frac{w_{ts} + w_{sp}}{2}\right) \tag{4}$$

$$x_5 = x_3 + x_1 = w_{tp} + w_{ts} \tag{5}$$

Where:

- w_{tp} is the width of the translator pole.
- w_{ts} is the width of the translator slot.
- w_{sp} is the width of the stator pole.
- w_{ss} is the width of the stator slot.

Table I summarises the results from studying the inductance profile:

Table I: Relationship between inductance profile and motor parameters

Rotor Position	**Results**
$0 - x_1$ and $x_4 - x_5$	No overlap between stator and rotor poles, position of minimum inductance and no force produced.
$x_1 - x_2$	Poles begin to overlap, the inductance increases with positive slope and a positive force is produced.
$x_2 - x_3$	Complete overlap of poles, no change in inductance thus no force produced. Allows for commutation.
$x_3 - x_4$	Poles start to move away from aligned position, inductance changes with a negative gradient and a negative force is produced.

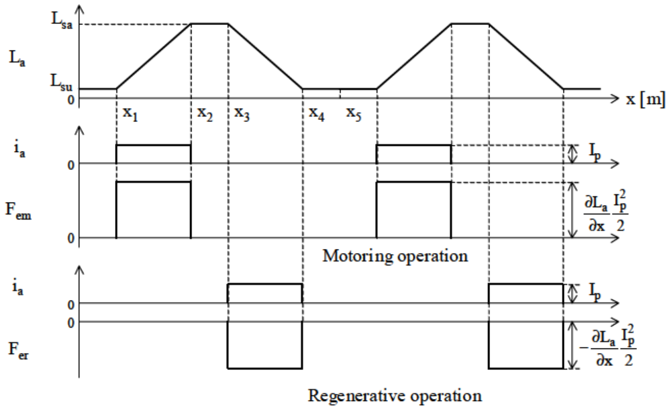

Figure 4: Inductance profile and force generation of LSRM

In figure 5, the forward motion is assumed to be positive when the sequence of phase excitation is abc. For forward direction of motion, regions I to III represent forward motoring operation and regions IV to VI represent forward regenerative operation for the phase sequence abc. Analogously, for reverse direction of motion, regions I to III represent reverse regenerative operation and regions IV to VI represent reverse motoring operation for the phase sequence acb. The duty cycle of each phase is only 1/3 and the induced emfs are constant between x_1 and x_2. P_{em} represents the motoring back emf power and P_{er} represents the regenerative back emf power. It should be noted that one half of the back emf is stored in the phase windings and the other half is converted into mechanical power output [2].

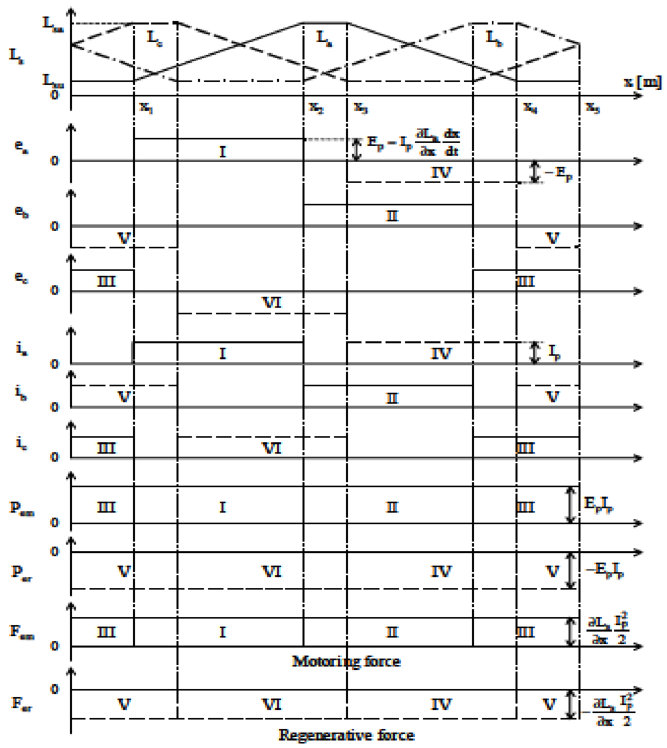

Figure 5: Operation of LSRM

The dynamic analysis of the motor gives the relationships between voltage, current, force and speed of the motor. The analysis is performed on the equivalent circuit of one phase of the motor only, reason being that the remaining phases have the same circuit. So, the results can be extrapolated for the other phases. Figure 6 shows the equivalent circuit of one phase of the LSRM. The following equations can be derived from the equivalent circuit:

The total magnetic flux vector $\lambda^T = [\lambda_1 \quad \lambda_2 \quad \lambda_3\,]$ of the motor is given as follows:

$$\lambda = L(x)i \qquad (6)$$

Where:

- i is the phase currents, and the vector is given as $i^T = [i_a \quad i_b \quad i_c\ ]$
- x is the position along the track.
- L(x) is the inductance matrix denoted as:

$$L(x) = \begin{bmatrix} L_{aa} & L_{ab} & L_{ac} \\ L_{ba} & L_{bb} & L_{bc} \\ L_{ca} & L_{cb} & L_{cc} \end{bmatrix} \qquad (7)$$

Where the main diagonal entries are the inductances of the respective phases and the other entries are the mutual inductances due to the coupling of the phases. The subscripts denote the phases.

Applying Kirchhoff's voltage law, the following is obtained:

$$V = Ri + L(x)\frac{di}{dt} + vi\frac{dL}{dx} \qquad (8)$$

Where:

- V is the phase voltage and is the same for all the phases, and the vector is given as $V^T = [v_a \quad v_b \quad v_c\ ]$.
- v is the speed of the motor.

The resistance matrix is given as follows:

$$R = \begin{bmatrix} R_a & 0 & 0 \\ 0 & R_b & 0 \\ 0 & 0 & R_c \end{bmatrix} \qquad (9)$$

Considering the equations obtained from the analysis, and applying the law of electrical machines, the general force equation is:

$$F = \frac{1}{2} i^T \frac{dL(x)}{dx} i \qquad (10)$$

If the mutual inductance due to coupling of the phases is ignored, then equation (7) becomes:

$$L(x) = \begin{bmatrix} L_{aa} & 0 & 0 \\ 0 & L_{bb} & 0 \\ 0 & 0 & L_{cc} \end{bmatrix} \qquad (11)$$

From (11), the induced force by the motor becomes:

$$F = \frac{1}{2}\left[i_a^2 \frac{dL_{aa}}{dx} + i_b^2 \frac{dL_{bb}}{dx} + i_c^2 \frac{dL_{cc}}{dx}\right] \qquad (12)$$

Furthermore, the dynamic behaviour of the motor can be expressed as:

$$F = m\frac{dv}{dt} + Bv + F_L \qquad (13)$$

Where:

- F is the motor induced force.
- m is the mass of the translator and load.
- B the damping coefficient.
- F_L the load force.

Combining all the above parameters, the state space model of the motor can be given as:

$$\begin{bmatrix} v' \\ i_a' \\ i_b' \\ i_c' \end{bmatrix} = \begin{bmatrix} -\frac{B}{m} & 0 & 0 & 0 \\ 0 & -\frac{K_{aa}}{L_{aa}} & 0 & 0 \\ 0 & 0 & -\frac{K_{bb}}{L_{aa}} & 0 \\ 0 & 0 & 0 & -\frac{K_{cc}}{L_{cc}} \end{bmatrix} \begin{bmatrix} v \\ i_a \\ i_b \\ i_c \end{bmatrix} + \begin{bmatrix} \frac{1}{m} & 0 \\ 0 & \frac{1}{L_{aa}} \\ 0 & \frac{1}{L_{bb}} \\ 0 & \frac{1}{L_{cc}} \end{bmatrix} \begin{bmatrix} F - F_L \\ V \end{bmatrix} \qquad (14)$$

Where:

- $K_{aa} = R_a + v\frac{dL_{aa}}{dx}$.

- $K_{bb} = R_b + v\frac{dL_{bb}}{dx}$.
- $K_{cc} = R_c + v\frac{dL_{cc}}{dx}$.

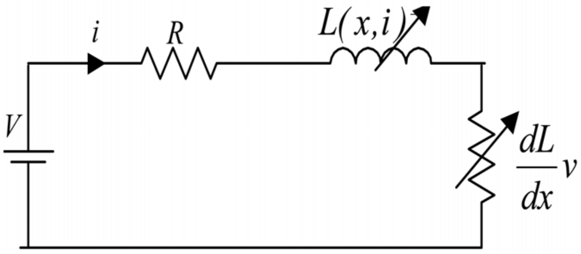

Figure 6:Equivalent circuit for one phase of the LSRM

3. DESIGN EQUATIONS

The equations used for the design of the LSRM are adapted from [2]. The design begins with designing an equivalent motor in the rotary domain and then converting it to the rotary domain. The following equations are used in the design of the motor:

$$F = ma \tag{15}$$

Where:

- F = force produced by the motor.
- M = total translator mass.
- a = the acceleration of the motor.

$$P = Fv \tag{16}$$

Where:

- P = rated motor power.
- v = the speed of the translator.

$$N_r = \frac{60v_m}{\pi D} \tag{17}$$

Where:

- N_r = is the rpm of the motor.
- V_m = speed of the RSRM.
- D = bore diameter of RSRM.

$$P = k_e k_d k_1 k_2 B_g A_{sp} D^2 L N_r \tag{18}$$

$$L = kD \tag{19}$$

Where:

- k_e = efficiency.
- k_d = duty cycle.
- $k_1 = \frac{\pi^2}{120}$.
- k_2 = variable depending on the point of operation.
- B_g = flux density of air gap in the aligned position.
- A_{sp} = the electric loading.
- L = stack length of magnetic core.
- k = constant multiple.

Substituting for N_r and L in the above equation and solving for the bore diameter, the following equation is obtained:

$$D = \sqrt{\frac{\pi P}{60 k_e k_d k_1 k_2 k B_g A_{sp} v_m}} \quad (20)$$

The machine flux linkage is given as:

$$\varphi = B_g A_g \quad (21)$$

Where:

- φ = flux linkage of motor.
- A_g = area of the air gap.

$$A_g = \left(\frac{D}{2} - g\right)\left(\frac{\beta_r + \beta_s}{2}\right) L \quad (22)$$

Where:

- g = length of the air gap.
- β_r = rotor pole angle.
- β_s = stator pole angle.

The magnetic field intensity of the air gap is given by:

$$H_g = \frac{B_g}{\mu_0} \quad (23)$$

Assuming that the air gap is sufficiently large, the ampere-turn required to produce the air gap magnetic field intensity is given as:

$$T_{ph} I_p = H_g \times 2g \quad (24)$$

Where:

- T_{ph} = number of winding turns per phase.
- I_p = maximum phase current.

Thus, for a given phase current, the number of turns per phase is given as:

$$T_{ph} = \frac{H_g \times 2g}{I_p} \quad (24)$$

Assuming that *J* is the maximum current density of the conductor, and *m* is the number of phases, then the cross area of the conductor is computed as follows:

$$a_c = \frac{I_p}{J\sqrt{m}} \quad (25)$$

By neglecting flux linkages, the following equations are obtained for the stator area, stator flux density, area of stator yoke and stator height:

$$A_s = \frac{D L \beta_r}{2} \quad (26)$$

$$B_s = \frac{\varphi}{A_s} \tag{27}$$

$$A_y = C_{sy} \times L = \frac{A_s B_s}{B_y} \tag{28}$$

$$h_s = \frac{D_0}{2} - \frac{D}{2} - C_{sy} \tag{29}$$

The corresponding equations for the rotor are:

$$A_r = \left(\frac{D}{2} - g\right) L\beta_r \tag{30}$$

$$C_{ry} = \frac{A_r}{L} \tag{31}$$

$$h_r = \frac{D}{2} - g - C_{sy} \tag{32}$$

The minimum stator and rotor arc can be selected by using the following equations:

$$\beta_s = \frac{4\pi}{P_s P_r} \tag{33}$$

$$\beta_r > \beta_s \tag{34}$$

Where:

- P_s = number stator poles.
- P_r = number of rotor poles.

The switching frequency in the phase windings is given by the following equation:

$$f_{sw} = 2P_r \frac{N_r}{60} \tag{35}$$

Equations (15) to (36) allow the design of the motor in the rotary domain. The following set of equations will then be used to convert from the rotary domain to the linear domain.
The bore circumference of the RSRM forms the length of one sector of the LSRM. The total number of sectors required for the LSRM is computed with the following equation:

$$N_{sc} = \frac{L_t}{\pi D} \tag{36}$$

The number of stator poles in the LSRM is obtained from the following equation:

$$n = P_s N_{sc} \tag{37}$$

The width of the stator pole and stator slot are given by:

$$w_{sp} = \frac{A_s}{L} = \frac{D}{2}\beta_s \tag{38}$$

$$w_{ss} = \frac{\pi D - P_s w_{sp}}{P_s} \tag{39}$$

The width of the translator pole and translator slot are given as follows:

$$w_{tp} = \frac{D}{2}\beta_r \tag{40}$$

$$w_{ts} = \frac{\pi D - P_r w_{tp}}{P_r} \tag{41}$$

The fill factor FF, is computed to verify that the slot size is sufficient to hold the windings, and is denoted as follows:

$$FF = \frac{Stator\ Winding\ Area}{Stator\ Slot\ Window\ Area} \tag{42}$$

The diameter of the conductor is given by:

$$d_c = \sqrt{\frac{4a_c}{\pi}} \tag{43}$$

Assuming that wedges given by w are put in in place to hold the windings, the number of vertical layers is given by:

$$N_v = f_f \frac{h_s - w}{d_c} \tag{44}$$

Where f_f is the packaging factor and $0.2 \leq f_f < 0.7$.
The number of horizontal layers is given by:

$$N_h = \frac{T_{ph}}{2N_v} \tag{45}$$

The stator winding area is given by:

$$Stator\ winding\ area = 2\frac{a_c N_v N_h}{f_f} \tag{46}$$

The stator slot window area is:

$$stator\ slot\ window\ area = w_{ss}(h_s - w) \tag{47}$$

Hence, the fill factor is given by:

$$FF = \frac{2a_c N_v N_h}{f_f w_{ss}(h_s - w)} \tag{48}$$

The motor that has been designed has 6 translator poles, thus the translator length of the LSRM is obtained from:

$$L_{tr} = 6w_{tp} + 5w_{ts} \tag{49}$$

The core stack length of the LSRM is obtained from the stator stack length of the RSRM:

$$L_w = L = kD \tag{50}$$

Once the design is done, the following condition must be satisfied in order to ensure that design is correct:

$$P_s(w_{sp} + w_{ss}) = P_r(w_{tp} + w_{ts}) \quad (51)$$

4. CONVERTER TOPOLOGIES

As per description of the operation of the LSRM, it is seen that excitation of the phase windings results in motion. Due to this excitation, the nearest rotor pole is pulled into a position of maximum inductance, where it aligns with the stator pole. Whilst the rotor is being pulled, a pull/push force is generated. The generated force is proportional to square of the current, consequently it is independent of the direction of the current [2]. From this, it can be realised that the current affects the force that is generated. As a result, the LSRM requires a converter to excite the phase windings, to change the operating frequency and applied voltage. There are quite a number of converter topologies that can be utilised for this application. The topologies differ by their regeneration method and number of switches used per phase [2].

When a single switch is used per phase, it can either be done with a bleeding resistor or with bifilar windings. The phase windings are excited, once the excitation current is turned off, then energy stored is either recovered through the bifilar winding or it dissipated in the resistor [2]. This is necessary to ensure that saturation does not occur. The commonly used converter topology has two switches per phase, as presented in figure 6. Both switches need to be closed simultaneously in order for an excitation current to pass through the phase [5]. When the switches are closed, the energy is stored in the form of a magnetic field. When the switches are off, the stored energy (regenerative process) is returned to DC supply through the diodes.

In order to protect the switching devices used in the converter, passive components can be placed in parallel with the switching devices. This protection method is called snubber circuit, and it also helps reduce switching losses [6]. The different types of switching devices that can be used are MOSFETs, IGBTs and BJTs.

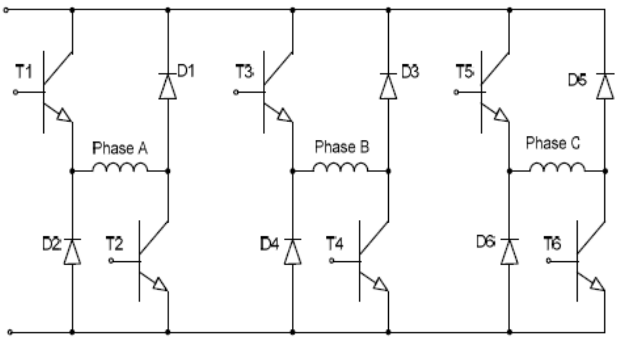

Figure 7: Asymmetric H-bridge converter

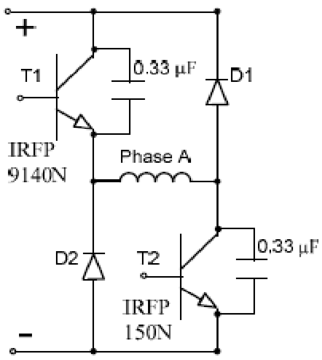

Figure 8: Snubber circuits for H-bridge converters

The following converter topology was used for this project because it reduces the number of components used as well as the complexity of the design.

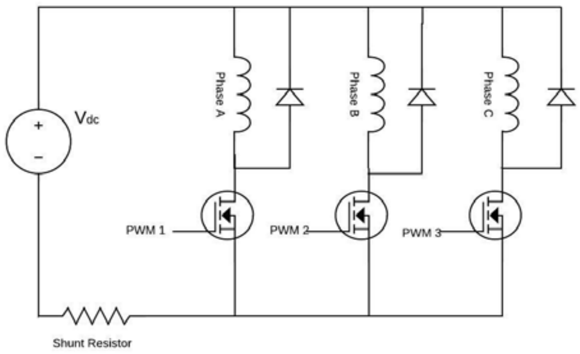

Figure 9: Modified convert for LSRM

5. CONTROL FOR LSRM

The dsPIC33FJ16GS502 microcontroller was used as the controlling unit for the LSRM, it has 16*kb* of memory. It has six PWM outputs, and six analogue input pins. The speed of the motor is computed from the outputs of the linear incremental position sensors; this is then used to calculate the PWM duty cycle for each conduction phase. The current sensor was implemented using the shunt resistors to measure the voltage across them. The measured voltage was amplified to a level the microcontroller could read using the LM328 operational amplifier. The output of the current sensors is used to ensure that correct current is maintained in each phase during each conduction phase. The IC has its own internal ADC, which simplifies the conversion of the sensor outputs. The following picture shows the implemented system:

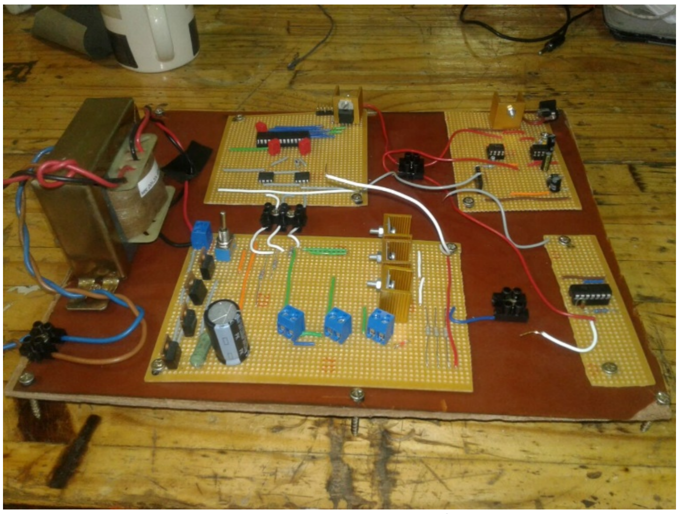

Figure 10: Implemented circuitry for the LSRM

6. CONCLUSION

The LSRM was designed and built successfully. The working principles of the LSRM were verified and found to be true. The motor was implemented using EI transformer laminations, so not much power was obtained to fully investigate the behaviour of the LSRM.

REFERENCES

[1] M. Thet, “Design and Calculations of 75W Three-Phase Linear Switched Reluctance Motor,” World Academy of Science, Engineering and Technology, no. 48, pp. 108-113, 2008.

[2] B.-S. Lee, Linear Switched Reluctance Machine Drives with Electromagnetic Levitation and Guidance Systems. Blacksburg, Virginia: Virginia Polytechnic Institute and State University, 2000.

[3] S. Abbasian, Simulation and Testing of a Switched Reluctance Motor By Matlab /Simulink and dSPACE, Göteborg, Sweden: Chalmers University of Technology, 2013.

[4] K. Praveen, K. Geetha and K. Madhavi, “Design, Modeling and Analysis of Linear Switched Reluctance Motor for Ground Transit Applications,” IOSR Journal of Electrical and Electronics Engineering (IOSR-JEEE), vol. 10, no. 1, pp. 1-10, 2015.

[5] M. Dursun, F. Koc, H. Ozbay and S. Ozden, “Design of Linear Switched Reluctance Motor Driver for Automatic Door Application,” International Journal of Information and Electronics Engineering, vol. 3, no. 3, 2013.

[6] C. Andersson, Design of a 2.5kW DC/DC Fullbridge Converter, Göteborg, Sweden: Chalmers University of Technology, 2011.

[7] M. Durssun and F. Koc, “Linear Switched Reluctance Motor Control with PIC18F452 Microcontroller,” in Turkish Journal of Electrical Engineering and Computer Science, 2013.

[8] Z. Wajdi, K. Jalel and R. Habib, “Modeling and Indrict Force Control of Linear Switched Reluctance Motor,” in International Conference on Control, Engineering & Information Technology (CEIT’14), 2014.

[9] P. kumar, K. Geetha and K. Madhavi, “Design, Modeling and Analysis of Linear Switched Reluctance Motor for Ground Transit Applications,” IOSR Journal of Electrical and Electronics Engineering (IOSR-JEEE), vol. 10, no. 1, pp. 1676-2278, 2015.

[10] R. Elevarasan, D. N. Lenin and D. R. Arumugam, “Analysis of Linear Switched Reluctance Motor Having Gashed Poles,” in IEEE, 2014.